

Structural and Biochemical Studies of FrzCD,  
A Cytoplasmic Methyl-accepting  
Chemosensory Protein (MCP)

A thesis submitted towards partial fulfillment of the requirements  
of the BS-MS Dual Degree Program



Submitted by,  
**JAZLEENA PJ**  
**20131033**

Research Mentor:

**Dr. Gayathri Pananghat**, Assistant Professor  
Biology Division, IISER Pune

Thesis Advisor:

**Dr. Amrita Hazra**, Assistant Professor  
Biology Division, IISER Pune



## CERTIFICATE

This is to certify that this dissertation entitled “Structural and Biochemical Studies of FrzCD, A Cytoplasmic Methyl-accepting Chemosensory Protein (MCP)” towards the partial fulfilment of the BS-MS dual degree programme at the Indian Institute of Science Education and Research, Pune represents study/work carried out by Jazleena PJ at IISER Pune under the supervision of Dr. Gayathri Pananghat, Assistant Professor, Department of Biology, IISER Pune during the academic year 2017-2018



Dr. Gayathri Pananghat  
Assistant Professor  
Department of Biology  
IISER Pune

Date: 20th March 2018



Jazleena PJ  
20131033  
Integrated BS-MS of the 2013 Batch  
IISER Pune

## DECLARATION

I hereby declare that the matter embodied in the report entitled “Structural and Biochemical Studies of FrzCD, A Cytoplasmic Methyl-accepting Chemosensory Protein (MCP)” are the results of the work carried out by me at the Department of Biology, IISER Pune under the supervision of Dr. Gayathri Pananghat and the same has not been submitted elsewhere for any other degree.



Jazleena PJ

20131033

Integrated BS-MS of the 2013 Batch

IISER Pune

Date: 20th March 2018



Dr. Gayathri Pananghat

Assistant Professor

Department of Biology

IISER Pune

## ABSTRACT

FrzCD is a Methyl-accepting chemotaxis protein (MCP) of *Myxococcus xanthus*. It was recently found to colocalize with the nucleoid and aid in the cooperative response of bacteria to signals. In vitro DNA binding studies suggested the sequence-independent DNA binding is by utilizing the N-terminal basic tail. MCPs have a sensor domain which is generally periplasmic for ligand binding, a HAMP linker to amplify and transmit the signal and a signaling unit to signal the downstream pathways. Our bioinformatic analysis has found out the presence of two contiguous HAMP domains in FrzCD. We aim to investigate the role of HAMP domains by systematic designing of domain deletion constructs and performing protein oligomerization and DNA-binding studies. Our preliminary results indicate that the higher order oligomerization of protein is mediated by the coiled-coil signaling unit. In the DNA-free state, HAMP domains restrict oligomeric state of the protein to a dimer. EMSA shows that coiled-coil domain stabilizes the protein-DNA complex possibly through a higher-order array formation. We are progressing further to quantify the binding affinities, to find the oligomeric state of the protein in the DNA-bound form and to obtain the crystal structure of the protein.

## LIST OF FIGURES

Figure number	Title of the Figure	Page number
1.1	The regulation of bacterial motility by chemosensory pathways	3
1.2	HAMP in signal amplification	5
1.3	Domain architecture prediction of FrzCD	6
2.1	Domain division of FrzCD	8
2.2	Stages of RF Cloning	11
2.3	Vapor diffusion method of crystalization	15
3.1	Cloning of all FrzCD constructs	16
3.2	Protein over-expression of FrzCD constructs	17,18
3.3	Protein preparation	19,20
3.4	Protein oligomerization studies	22
3.5	DNA binding assays with 429 bp DNA	25
3.6	DNA binding assays with 69 bp DNA	26
3.7	DNA binding assays with 35 bp DNA	27
3.8	DNA binding assay of DB-H1-H2 with a plasmid DNA	27
3.9	Crystals of FrzCD	31

## LIST OF TABLES

Table number	Title of the Table	Page number
2.1	Primers designed for FrzCD constructs	9
2.2	PCR conditions	9
2.3	PCR cycle	10
2.4	DNA used for EMSA	14
3.1	Molar mass estimation from SEC-MALS	23
3.2	Crystallization conditions	28

## TABLE OF CONTENTS

Sections	Page number
<b>Chapter 1. Introduction</b>	1
1.1 <i>Myxococcus</i> life cycle and motility	1
1.2 FrzCD, the major regulator of motility	1
1.3 Structure and function of MCPs in bacterial Motility	2
1.4 Role of HAMP in signal amplification	3
1.5 Proposed domain architecture of FrzCD	5
1.6 Objectives	7
<b>Chapter 2. Materials and Methods</b>	8
2.1 Design of the different constructs of FrzCD	8
2.2 Cloning by Restriction-Free (RF) Method	8
2.3 Protein expression and solubility	11
2.4 Protein purification	12
2.5 DNA binding assay by EMSA	13
2.6 Oligomerization studies by SEC-MALS	14
2.7 Crystallization by vapor diffusion	15
<b>Chapter 3. Results</b>	16
3.1 Cloning	16
3.2 Overexpression of Proteins	17
3.3 Protein purification	18
3.3 Protein Oligomerization States	21
3.4 DNA binding assays	24
3.5 Crystallization by trials of FrzCD.wt	28
<b>Chapter 4. Discussion</b>	32
<b>Chapter 5. Conclusion and Future plans</b>	36
<b>Chapter 6. References</b>	37

## ACKNOWLEDGEMENTS

As I approach towards the completion of my BS-MS, I realize that my lab had a crucial role in my academic as well as personal life. The knowledge I have acquired from the lab is deeper than any coursework had given me. Foremost, I would like to express my sincere gratitude to Gayathri Ma'am who gave me great opportunities to carry out fascinating projects for the past three years. She was always encouraging and caring. I am grateful to Dr. Saikrishnan Kayarat for his constant support and thought-provoking comments throughout the project discussions. The common lab meetings we had among both the labs was a good platform to discuss the projects and share the ideas among each other. I thank Dr. Amrita Hazra for listening to my project, for her valuable advices as my TAC member and also for her inspiring lectures during the coursework.

I express my gratitude to Dr. Radha Chauhan, Pravin Devangan for all the help during the SEC-MALS runs done in NCCS. I would like to thank Yaikhomba Mutum for all the previous work carried out in this project and for the initial helps with experiments when I moved into the FrzCD project.

I express my deep gratefulness to Ishtiyag Ahmad, who always used to give me good inputs whenever I got stuck in my experiments. He had found time to discuss my project even in his busy schedule. I'm much obliged to Mahesh bhaya and Sujata dee who were always ready to give suggestions and support whenever I needed.

It is most important that you need a person to guide you and make you learn the initial experiments and basic techniques in the lab. I express my heartfelt thanks to Priyanka dee for taking care of me in my initial lab days. I am also grateful to Jyoti dee, Shrikant bhaya and Mrinmayee for making me perform my experiments without many mistakes.

Everyone in the lab was very helpful and cooperative. The lab was filled with peace and joy because of this kind and generous behavior of every individual. I express my love and gratitude to all the G3 and SK lab members. I specially thank Pratima and Manil who always helped me and supported me in all my troubles. I also thank Suman Pal for being the part of my project and helping in different stages of it.

Thanks to Dr. Gregor for his great inspiration and motivation which gave me a positive energy. I thank my friends Aathira, Aiswarya. MS, Joyeeta and Basila who were always with me in all the peaks and valleys of my life. I extend my thanks to my beloved parents who always supported me.



# 1. INTRODUCTION

## 1.1 *Myxococcus* life cycle and motility

*Myxococcus xanthus*, a gram-negative bacterium, lacks flagella and hence glides on solid surfaces. These cells grow and divide and search for prey in nutrient-rich condition. They form a fruiting body by aggregating to a focal center under nutrient starvation. They enter into a stage of dormancy and are resistant to environmental stress until next favorable condition arises (Zusman et al., 2007). There are two motility control systems in *M. xanthus*. The movement of single cells are controlled by the adventurous (A) motility and the group movements are coordinated by the social (S) motility system. S-motility is determined by the assembly of type IV pili at the leading pole. A-motility is governed by the focal adhesion complexes (Zusman et al., 2007). During the normal growth phase, the cooperative swarming movement of the bacteria helps in the production of digestive enzymes and antibiotics and thus facilitates predation. These cells are found to have periodic reversals during predation for the efficient utilization of resources. The directed movement of the cell towards attractants like peptides, yeast extract and away from the repellents such as DMSO proved that *M.xanthus* do exhibit chemotaxis behavior (Shi et al., 1993). FrzCD, the homolog of *E.coli* MCP is found to be highly methylated in the presence of attractants and demethylated in response to repellents (Bustamante et al., 2004).

## 1.2 FrzCD, the major regulator of motility

The *frz* pathway consists of a set of seven genes (*frizzy* genes) which were initially identified from those mutants of *M. xanthus* that form frizzy filaments instead of fruiting bodies under starvation. Further studies revealed that these genes are the key determinants of frequency of reversals in the cell. Most of the *frz* mutants were not able to reverse the cells but *frzCD* mutant was showing no net movement since it had a hyper reversal phenotype.

FrzCD - a sensor protein, FrzE - a histidine kinase, FrzF- a methyltransferase and FrzG - a methylesterase, FrzZ - a response regulator and FrzA, FrzB - CheW homologs constitute the pathway (Figure 1.1A). FrzCD activates the

autophosphorylation of FrzE and this leads to the phosphorylation of FrzZ. FrzCD is found to be involved in the cross-talk between the cells and help in coordinated ripple movement of the bacteria during swarming (Guzzo et al., 2015).

### **1.3 Structure and function of MCPs in bacterial motility**

Methyl-accepting chemotaxis proteins (MCP) help bacteria to sense the environmental cues and thus enable them to respond to attractants/repellents in the surroundings. The role of MCP is to bind to the chemo-attractants/repellents and convey this signal to downstream pathways. The three major domains of the MCPs are (1) the sensory domain (2) the HAMP linker domain, and (3) the signaling domain. Although the topology of sensory domain can be either periplasmic or cytoplasmic, the HAMP and the signaling unit are always found in the cytoplasm of bacteria (Alexander, 2007).

MCPs contain a long coiled-coil domain, which gets methylated and hence is termed as the signalling domain. They form homodimers. Transmembrane MCPs form hexameric arrays by arranging themselves in the membrane as trimer of dimer assemblies (Hall *et al.*, 2012). While crystal structures of homodimeric coiled coil domains of MCP (PDB IDs: 2CH7, 3ZX6) are available, the hexameric assemblies have been observed only in vivo using cryotomography (Briegel *et al.*, 2011).

The *E.coli* MCPs Tsr, Tar, Tap, and Tag have a periplasmic sensory domain and Aer has a cytoplasmic sensory domain. All of these five MCPs signal down to a single Che-pathway to control the flagellar motor (Figure 1.1B). Upon signal sensing, the MCP induces autophosphorylation of CheA through an adaptor protein CheW. CheA, in turn, phosphorylates CheY which causes the tumbling of cell and redirection of motion (Wadhams and Armitage, 2004). When there are repellents or decreased concentration of nutrients, the glutamate residues in the C-terminal coiled-coil domain of MCP gets methylated. This state is responsible for activation of downstream pathways. When the histidine kinase CheA gets activated, it phosphorylates CheB which demethylates the MCP. Now, if the MCP has to get activated again, it should sense a further low nutrient concentration (Wadhams and Armitage, 2004) .

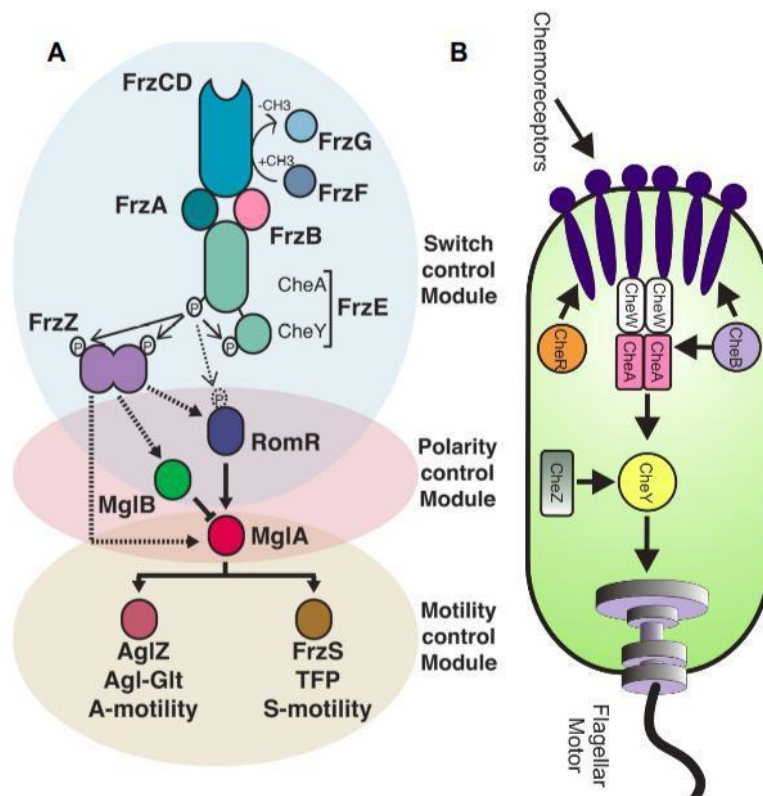


**Figure 1.1. The regulation of bacterial motility by chemosensory pathways (A )Frz pathway proteins controlling motility of *Myxococcus xanthus*. Adapted from ( Mauriello EMF, et al (2015) (B) Che proteins that regulate the flagellar movement in *E. coli*. Adapted from [www.2011.igem.org/Team:WITSCSIR\\_SA/Project/Motility](http://www.2011.igem.org/Team:WITSCSIR_SA/Project/Motility)**

## 1.4 Role of HAMP in signal amplification

The HAMP linker domain was named so because it was initially identified in histidine kinases, adenylyl cyclases, methyl-accepting chemotaxis proteins (MCPs), and phosphatases. The major role of HAMP is to transmit the signals from the sensing domain to the signaling unit. A single HAMP unit (~ 50 amino acid residues) comprises two amphipathic alpha-helices AS1 and AS2, and a flexible linker (~ 14 amino acid residues) which separates the two. A heptad repeat of a-g, where positions 'a' and 'd' forms the hydrophobic core is a feature of these alpha helices which is very similar to the coiled-coil (Alexander, 2007).

The mechanism of signal transduction by HAMP domain has been a long-standing question for structural biologists and various models were proposed on the basis of

available structural and biochemical studies. This includes dynamic bundle model, gearbox model, lever-like motions and scissoring model. The crystal structure of Aer2 receptor (PDB ID: 3LNR) reveals how three consecutive HAMP domains form a di-HAMP unit (Airola et al., 2010). In this “concatenated di-HAMP unit”, the AS2 of HAMP1 is continuous with the AS1 of HAMP2 and AS2 of HAMP2 is continuous with the AS1 of HAMP3. It is proposed stutter compensation may result in the formation of a kink at HAMP2/3 junction (Airola et al., 2010).

The complete structure of the sensor histidine kinase NarQ both in ligand-bound and ligand-free states was published recently (PDBID: 5IJI, 5JEF, 5JEQ) (Gushchin et al., 2017). The transmembrane domain and the signaling domain is linked by a single HAMP domain. A slight displacement (0.5-1Å ) of the sensor upon ligand-binding is translated into a piston-like movement by TM domain (7 Å) and is further amplified by the lever-like rotation of HAMP unit which finally leads to a 90° helical rotation that destabilizes the signaling unit. In the ligand-bound form, the AS2 of adjacent dimers are found to be interfused with each other which may help in the formation of higher order oligomers. The structural flexibility of HAMP is utilized by the system for signal amplification as well as oligomerization.

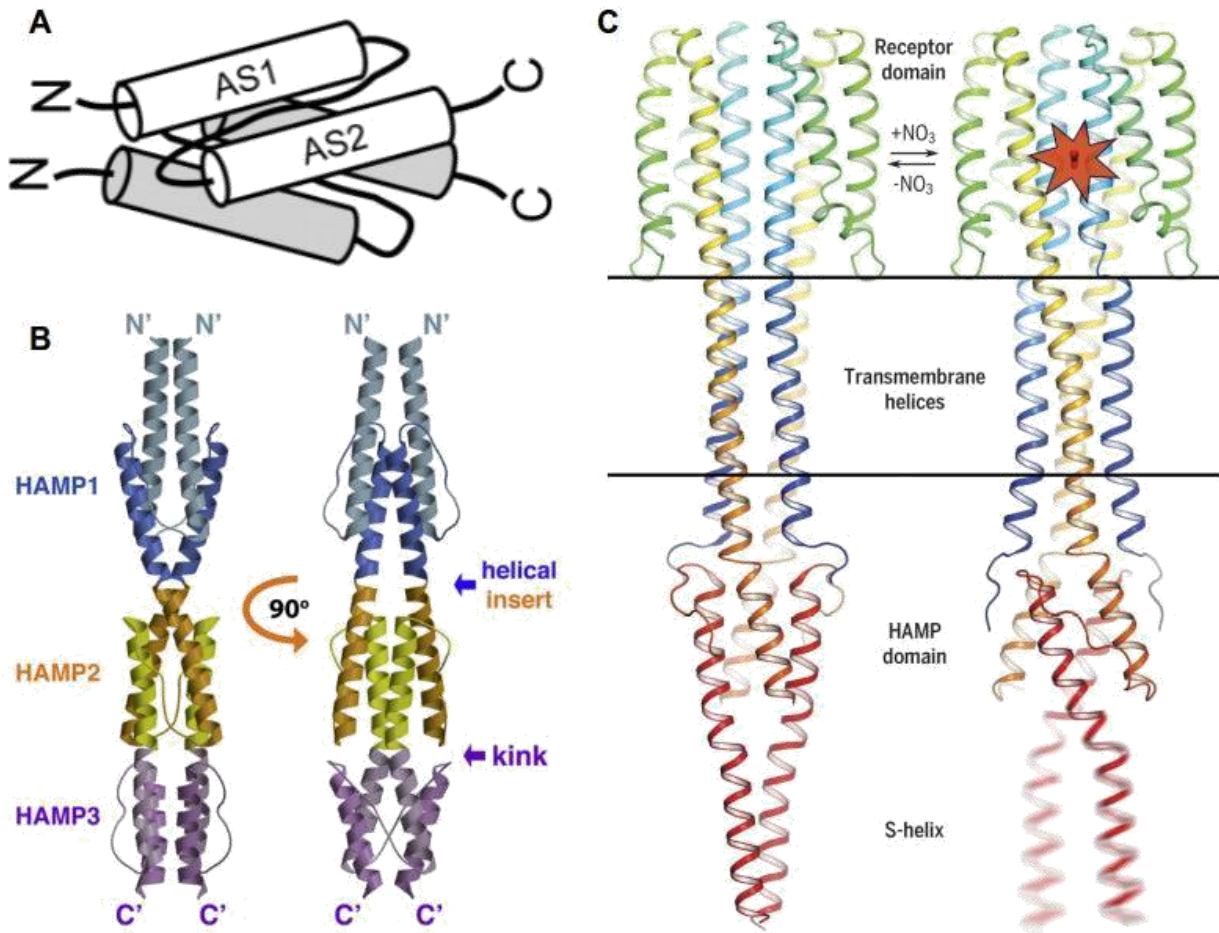


**Figure 1.2: HAMP in signal Amplification.** (A) The four helical bundle arrangement of HAMP in a dimer. (B) Concatenated di-HAMP unit. (C) The complete crystal structure of MCP in ligand-free and ligand-bound form. Figure panels adapted from Alexander, 2007; Airola et al., 2010; Gushchin et al., 2017.

## 1.5 Proposed domain architecture of FrzCD

FrzCD is a cytoplasmic MCP, unlike many other MCPs which have periplasmic sensor domains. The signaling unit of FrzCD, the C-terminal coiled-coil region is very well characterized. The N-terminal domain of FrzCD was predicted to be the ligand-binding region. Earlier findings from our lab had shown that N-terminal domain has a DNA binding function. The DNA binding is sequence independent. A stretch of positively charged lysines and arginines were found in the N-terminus of the protein. It is hypothesized that these residues might be involved in binding to the phosphate backbone of DNA. Sequence alignment of FrzCD with other MCPs has revealed the presence of two HAMP domains in

the protein (Yaikhomba Mutum, MS thesis 2017) (Figure 1.3A). The function of HAMP domain in the protein has not been characterised before, and the presence of two tandem HAMP domains was newly identified. The secondary structure prediction shows that the AS2 of HAMP1 is continuous with the AS1 of HAMP2 of FrzCD. This indicates the presence of a di-HAMP unit in FrzCD similar to that of the reported Aer2 receptor. Thus we propose the domain architecture of FrzCD as N-terminal DNA binding region followed by a concatenated di-HAMP unit composed of HAMP1 and HAMP2 and a long C-terminal coiled-coil signaling domain (Figure 1.3C).

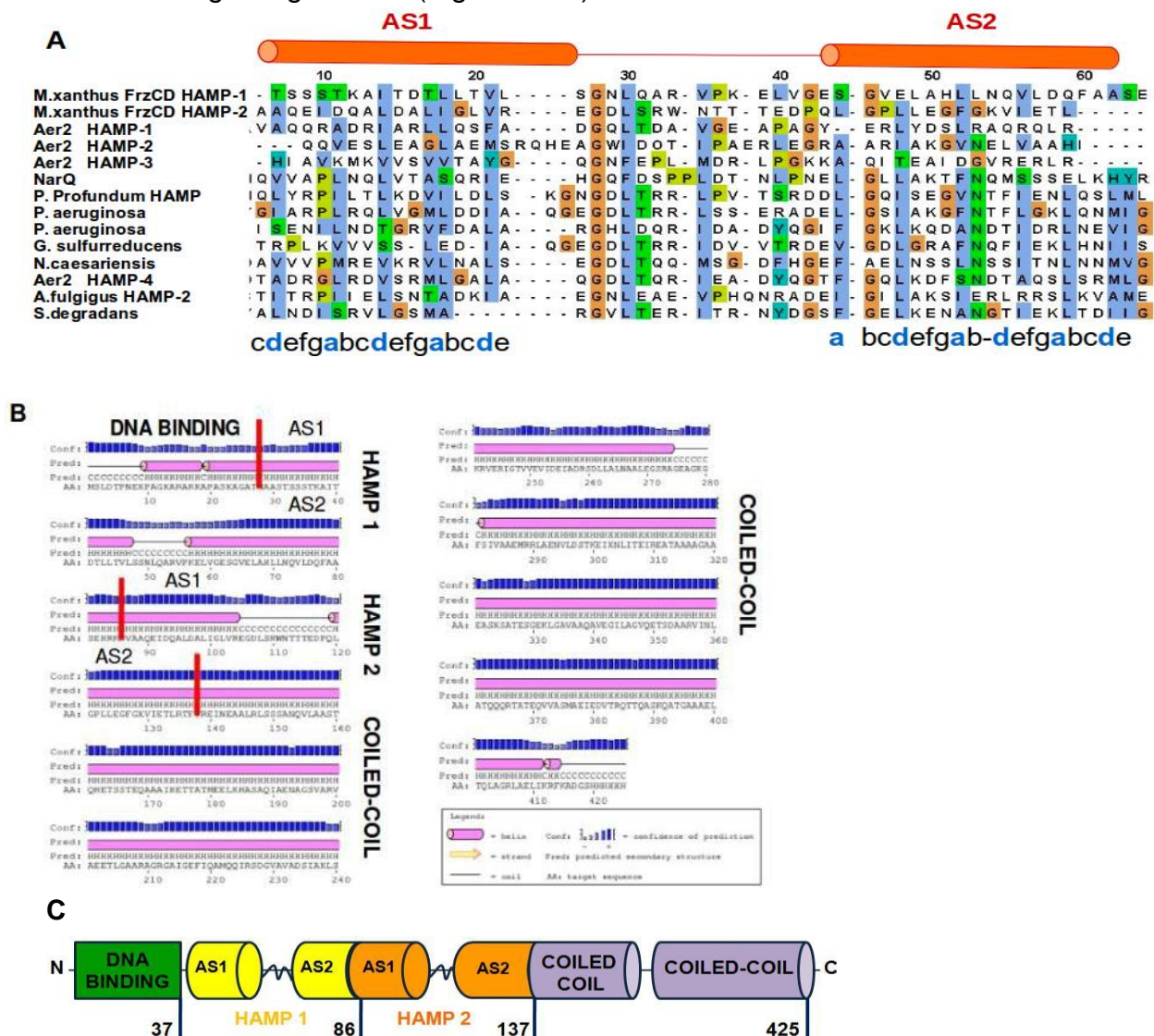


**Figure 1.3: Domain Architecture prediction of FrzCD.**(A) Sequence alignment of FrzCD HAMP1 and HAMP2 with other well known HAMP domains. (B) Secondary structure prediction of FrzCD sequence using PSIPRED (C) Predicted domain architecture of the protein

## 1.6 Objectives

HAMP domains are majorly involved in signal amplification and oligomerization for the well known MCPs (Gushchin et al.,2017) They serve as a flexible connector for the transmission of signals from the periplasm to the cytoplasm. The presence of HAMP domain in FrzCD was an interesting fact since it was a completely cytoplasmic MCP. The role of HAMP in FrzCD was never analyzed before. The in-vitro DNA binding and in-vivo colocalization experiments suggest that FrzCD acts cooperatively. We aim to investigate the role of HAMP domain in cooperativity and oligomerization of the protein.

The specific objectives of the project include:

- To understand the role of HAMP domain
  1. Design of different domain deletion constructs of FrzCD.
  2. Cloning, over-expression and purification of proteins.
  3. Oligomerization studies using SEC-MALS.
  4. DNA binding assays by EMSA with different length of DNA
  
- Crystallization of FrzCD.wt to get the real picture of the domain architecture and other residue interactions which helps in protein oligomerization

## 2. MATERIALS AND METHODS

### 2.1 Domain architecture prediction of FrzCD

The alignments with HAMP domains of other MCPs were done using Jalview software. Secondary structure of the protein was done using Psipred (<http://bioinf.cs.ucl.ac.uk/psipred/>).

### 2.2 Cloning by Restriction-Free (RF) Method

A Restriction-Free (RF) PCR was used for cloning all the constructs into pHis17 vector (van den Ent & Löwe, 2006).

#### Primer Design:

For the DB-H1-H2 construct, we had to truncate the protein at 137 amino acid residues. A reverse primer for the corresponding DNA sequence was designed flanking with BamH1 restriction site and 6xHis-tag at the end. DB-H1-CC, DB-H2-CC and DB-CC had to be cloned by deleting the intermediate domains (Figure 2.1). The primers were designed such that it has a complementary sequence at the end of one domain and the beginning of the next domain excluding the sequence from the unwanted domain. The primers used in the study are tabulated (Table 2.1).

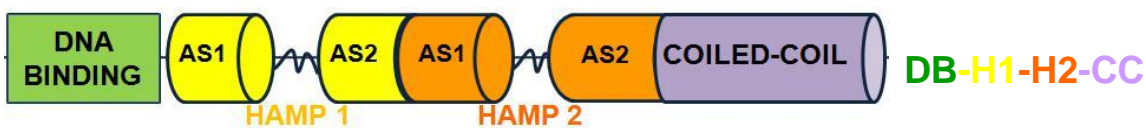


**Figure 2.1:** Domain division of FrzCD



**Table 2.1:** Primers used for cloning different constructs of FrzCD

Primer Name	Sequence
EFCD-f	5'-CC CCC AAC GAG <b>GAG</b> CCGCTGGC <b>GAG</b> GCT <b>GAA</b> GCC <b>GAGGAG</b> GCCCCCGCCTCC <b>GAG</b> GCC GCG GCC- 3'
DB-H2-CC	5'-GGCGCCACGAACGCGGCGTC <b>GCGCAAGCATGTGGCGGCG-3'</b>
DB-CC	5'-GGCGCCACGAACGCGGCGTCGGTGCGGGAGATCAACGAG-3'
DB-H1-CC	5'- <b>CAGTTCGCGGCCTCCGAGCAC</b> GTGCGGGAGATCAACGAG-3'
DB-H1-H2-r	5'-GCTTTTAATGATGATGATGATGATGGGATCC <b>GAA</b> <b>GGTGCGCAGCGTCTCGATG-3</b>

**RF Cloning strategy:**

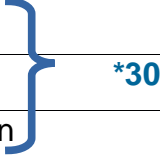
A Polymerase Chain Reaction (PCR) was done for the initial amplification of the gene of interest (Tables 2.2 and 2.3). FrzCD.wt clone was used as the template. Along with the designed primer for the deletions, vector specific forward/reverse primers were used accordingly (Figure 2.2).

**Table 2.2 :** PCR conditions

Components	Final Concentration	Volume ( $\mu$ L)
PrimeSTAR GXL DNA Polymerase	0.625 U	0.5
Buffer (10x)	1x	5
dNTP mix (10mM each)	0.2 mM	1
Template (330 ng/ $\mu$ L)	100 ng	0.3
Forward Primer (20 $\mu$ M)	0.4 $\mu$ M	1
Reverse Primer (20 $\mu$ M)	0.4 $\mu$ M	1
MilliQ		41.2

**Table 2.3 : PCR cycle**

Step	Temperature ( °C)	Time
Initial Denaturation	95	30 sec
Denaturation	95	30 sec
Annealing	60	40 sec
Extension	68	1 kb/min
Final Extension	68	5 min
Hold	4	



The PCR product was checked by loading 2  $\mu$ L on 0.8% agarose gel along with a DNA ladder. If there was no amplification or the product was smeary in the gel, the same reaction was repeated using a gradient PCR, where the annealing temperature was varied. The 50  $\mu$ L reaction mixture was divided equally into 5 tubes and each of them was treated with different annealing temperatures ranging from 55 °C - 68 °C The PCR product showing a single amplified band of the expected size was purified using PCR purification kit (Qiagen). If there was more than one band, the PCR product was subjected to purification of the desired band size through gel extraction. The whole sample was loaded onto a 1% agarose gel run at 90 V and the separated single band of interest was cut out from the whole gel. The DNA was purified from the gel using the Qiagen Gel extraction kit. 1  $\mu$ g of this purified DNA was used as a primer pair for the Restriction-Free PCR reaction. The parental plasmid which is methylated can be digested by Dpn1 digestion. 9.5  $\mu$ L of RF PCR reaction mixture and 0.5  $\mu$ L Dpn1 enzyme was incubated at 37 °C for 3 hrs. It was then transformed into NEB turbo Chemically competent cells by heat shock method. The cells were spread onto Luria-Bertani (LB) broth Agar plates with ampicillin at 100 g/ml. The plates were incubated at 37 °C and checked after 9 -12 hrs. Single colonies were inoculated into Luria-Bertani (LB) broth with 0.1 mg/ml ampicillin and grown for 8-12 hrs. Cells were pelleted down and the plasmid isolation was done using QIAprep Spin Miniprep Kit of Qiagen. Gene insertion of the truncated constructs into pHis17 vector was verified

by a digestion check with NdeI and BamHI restriction enzymes. The 10  $\mu$ L reaction mixture consists of 0.5  $\mu$ L of each enzyme, 1  $\mu$ L of 10x cut smart buffer and 150 ng of plasmid. Clones were further confirmed by sequencing by single pass DNA sequencing method.

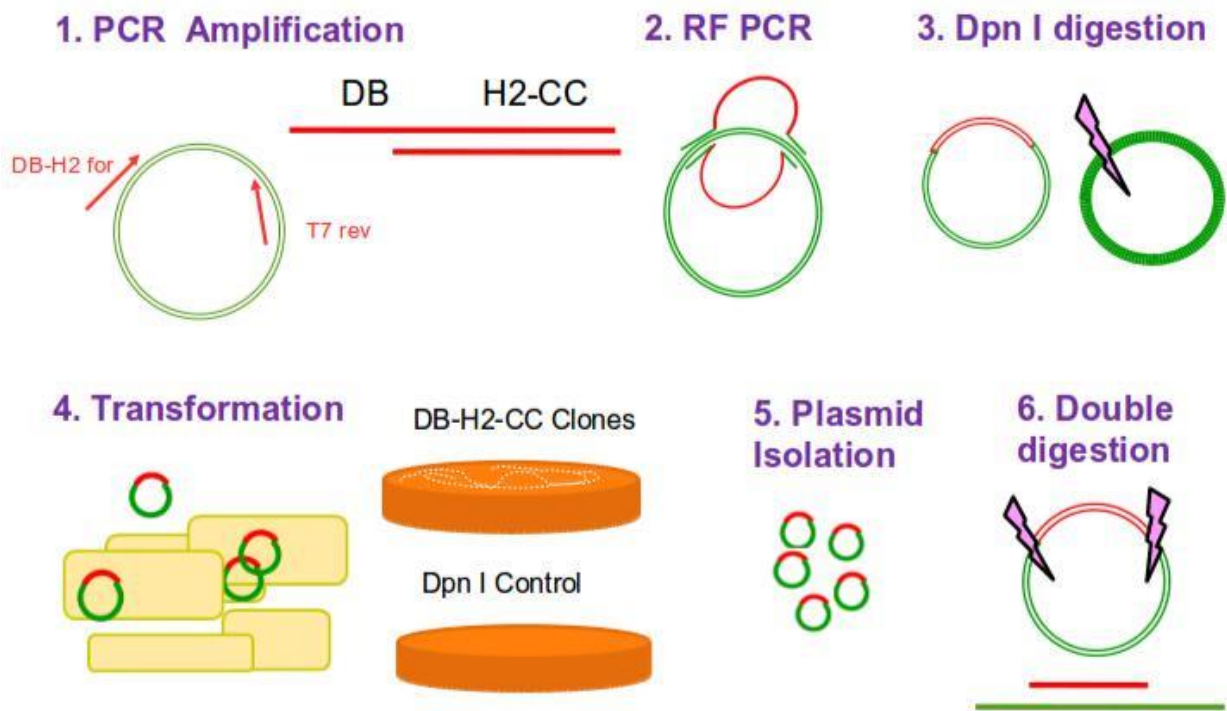


**Figure 2.2:** Stages of RF Cloning. (An example with DB-H2-CC is shown)

## 2.3 Protein Expression and Solubility

For over-expression of protein, the clones were transformed into BL21-AI and BL21-DE3(C43) (Invitrogen) strains of *E. coli*. A patch of colonies was grown in 11 ml LB media with ampicillin selection at 37 °C till the OD<sub>600</sub> value reached 0.8-1. The cultures were divided into 5 ml each and one of them was kept as uninduced along with the induced under the same conditions of incubation. BL21-AI and BL21-DE3(C43) cell cultures were induced with 0.2% L-arabinose and 0.5 mM IPTG respectively. The cultures were grown at 30 °C for 6 hrs post induction. These were pelleted down and resuspended in lysis buffer (200 mM NaCl, 50 mM Tris pH-8.0, 10% glycerol). It was sonicated (Sonics VibraCel) in a 5" ON and 5" OFF cycle at 60% amplitude for a total time of 1 minute.

From the sonicated solution, 20  $\mu$ l was taken and mixed with 20  $\mu$ l of 2xSDS dye which will show the total expression of a protein in the cell. It was centrifuged at 21130 g-force and the resultant supernatant sample was also similarly mixed with SDS dye. 20  $\mu$ l of this sample was loaded onto 12% SDS-PAGE gel for all the constructs and 15% gel for DB-H1-H2 which is a 15 kDa protein.

## 2.4 Protein Purification

Protein preparation was done by affinity chromatography (HisTrap, GE Life Sciences) followed by an ion-exchange chromatography and in all the stages temperature was maintained as 4 °C. For protein purification, the cultures were grown in the well-expressed strains in large scale according to the level of expression of each construct (500 mL – 4 L). A primary culture of 50 mL was grown by inoculating from a 12 hr plate of the transformed cells. When OD<sub>600</sub> was 0.8, 1% of the primary culture was inoculated into 500 ml growth medium in a 2L conical flask. It was induced when OD<sub>600</sub> was 0.8-1 and grown for 6 hrs post induction at 30 °C. The cultures were pelleted down. It was flash frozen in liquid nitrogen and stored in -80 °C freezer.

A one-litre culture pellet was resuspended in 60 mL lysis buffer. It was lysed by a sonication cycle of 1" ON and 3" OFF for a total time of 2 minutes. This was repeated thrice with interval of 5 minutes. It was spun for 45 min at 39, 191 g-force. A 5-ml HisTrap TM FF (GE Healthcare) column was initially washed with Buffer-B (500 mM imidazole, 200 mM NaCl, 50 mM Tris pH-8.0) and equilibrated with Buffer-A ( 200 mM NaCl, 50 mM Tris pH-8.0). The supernatant was passed through the column and flow-through was collected at the same time. It was followed by excessive wash by passing 8 column volumes (40 ml) of 2% and 5% of Buffer-B. The fractions were collected by increasing the percentage of Buffer-B in a step-wise manner (10%, 20%, 50%, 100%). For every concentration of B, 6 fractions of 5 mL each were collected. The supernatant, flowthrough, wash and the alternate fractions were loaded onto SDS-PAGE gel to identify the fractions that contained pure protein. The fractions with protein were pooled together and dialyzed for 2 hrs in A-50 (50 mM NaCl, 1mM EDTA, 50 mM Tris pH-8.0 ) buffer to lower the salt concentration. It was filtered and loaded onto Mono Q-PE 10/100 GL (GE Healthcare) for performing Anion Exchange Chromatography. This step helped to remove bound nucleotides and DNA

along with other impurities. Protein was loaded with buffer containing 50 mM NaCl and eluted by a gradient of increasing salt concentration from 50 mM to 335 mM.

Fractions containing protein were concentrated using centricons (Vivaspin® 10 kDa MWCO). FrzCD.wt protein was diluted into A-50 buffer to maintain the salt concentration, especially for samples used for crystallization. Concentrated protein was aliquoted into thin-walled PCR tubes, flash frozen with liquid nitrogen and stored in -80 °C freezer.

## 2.5 DNA binding assay by EMSA

Electrophoretic Mobility Shift Assay (EMSA) is an efficient technique for visualizing protein-DNA interactions. Migration of DNA through the gel depends on molecular weight and shape. When the protein forms a complex with DNA, the molecular weight increases which leads to the retardation in mobility of protein-DNA complex compared to the free DNA. Samples with increasing concentrations of protein with a constant DNA concentration were used to qualitatively estimate the binding affinities. It was incubated in a binding buffer at 25°C for 30 minutes. The binding buffer consists of 50 mM NaCl, 1 mM DTT, 50 mM Tris pH-7.4 and 10% glycerol. The details of the binding assays including the DNA sequences of varying lengths are summarised in Table 2.4. For the ease of addition and to reduce pipetting errors, a master mix was made for 10 reactions which contains:

10 µL 10x buffer ( 500 mM NaCl, 10 mM DTT, 500 mM Tris pH-7.4)

20 µL 50% Glycerol

10 µL DNA (400 nM for 300 bp, 5 µM for 70 bp, 10 µM for 35 bp)

10 µL MQ (filtered deionized water )

For a 10 µL reaction, 5 µL of this master mix was added and the rest of the volume was made up of protein (from 0 – 50 µM) and MQ.

**Table 2.4:** DNA used for EMSA

Length of DNA used	Concentration (nM)	Agarose Gel (%)	Sequence (5' --> 3')	GC content (%)	Molecular weight (Da)
35	1000 nM	3.5 %	GTCACCTGCTCTAGCTAATAGACTGAGCCGAGGTG	54 %	21504
69	500 nM	2.5 %	CTTGCAGTAGAGCTGACCATGATTACGCCATCAGCA GCTCCAGGTCGTACCTCCAGCTACCAATCCCCG	57 %	42515.6
429	40 nM	1.5 %	TAATACGACTCACTATAGGGAGACCACAACGGTTTCC CTCTAGAAAATAATTTTGTTTAACTTTAAGAAGGAGATA TACATATGTCCCTGGACACCCCCAACGAGAAGCCCCG CTGGCAAGGCTCGCGCCCGGAAGGCCCCCGCCTC CAAGGCCGGCGCCACGAACGCGGCGTGCACCTCTT CCTCCACCAAGGCCATCACCGACACGCTGCTGACG GTGCTGTCCGGCAACCTGCAGGCCCGCGTGCCCAA GGAGCTGGTCGGTGAGTCCGGCGTGGAGCTGGCG CACCTGCTCAACCAGGTGCTGGACCAGTTCGCGGC CTCCGAGCACCGCAAGCATGTGGCGGCGCAGGAGA TCGACCAGGCGTTGGATGCGCTCATCGGCCTGGTG CGCGAGGGCGGATCCCATCATCATCATCATTAAA AGC	61 %	265159.67

## 2.6 Oligomerization studies by SEC-MALS

Size Exclusion Chromatography (SEC) separates the molecules according to their hydrodynamic radius. The molecules with bigger molecular size elute first and those with lower size elute later. Thus the elution depends on the molecular size of the oligomeric state in solution, and not on the monomeric molecular weight. The volume of elution also depends on the shape of the molecule, and size estimation using SEC is accurate only for globular proteins. So when it comes to the molar mass estimation, we may not get accurate data for coiled-coil proteins, unlike the globular proteins.

Light scattering enables to get properties of biomolecules in solution (Folta-Stogniew and Williams, 1999). It does not require other calibration curves with different molecules. This technique measures the intensity of scattering and calculates the molar mass and rms radius in solution rather than relying on the elution volume from the column. We used Superdex 200 Increase 10/300 GL column for the SEC-MALS connected to an Agilent HPLC having 18-angle light scattering detector (Wyatt Dawn HELIOS II) and a refractive index detector (Wyatt Optilab T-rEX). The Zimm model implemented in ASTRA software was used for the curve fitting, and estimation of molecular weights. BSA at 2 mg/ml was used for calibration of the system.

## 2.7 Crystallization by Vapor diffusion

Sitting drop and hanging drop techniques of vapor diffusion method were used for crystallization trials. Generally, the protein concentration was 6 mg/ml and varied for different optimization trials. For sitting drop, a 48-well (8\*6) crystallization plate having a reservoir and a space for addition of the protein and crystallization condition mix as a drop was used. The reservoir was filled with 85  $\mu\text{L}$  of the condition. The 1  $\mu\text{L}$  drop was set-up in different protein:crystallization condition ratios (1:1, 1:2, 2:1). It was kept in 18 °C incubators and allowed to equilibrate. As the excess water in the drop vaporizes slowly, the protein-reagent concentration increases. When the protein reaches a supersaturation stage along with the optimum combination of reagents, it forms crystals. The plates were observed under microscope regularly after two days of incubation.

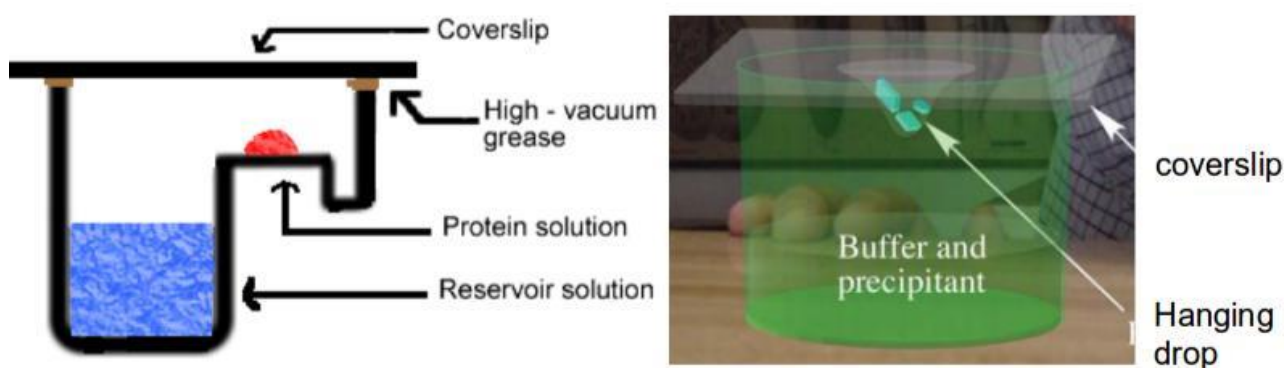


**Figure 2.3:** Sitting drop and Hanging drop set-up of vapor diffusion method of crystal growing. (Adapted from Rhodes, 2003)

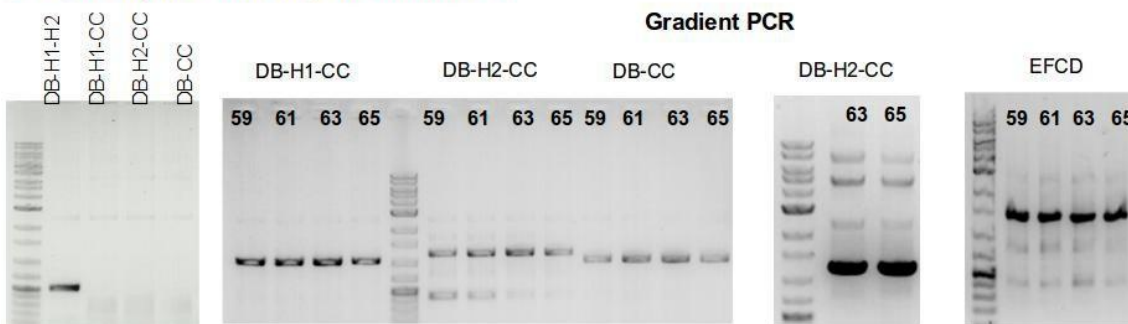
Additive Screen HTTM- HR2-138 and Silver Bullets-HR2-096 was set-up in a 96 well (8\*12) plate for further optimization of the hits. The 10% of reagent from this kit was manually added to the parent condition. A 400 nL sitting drop consisted of 200 nL protein and 200 nL condition and the reservoir had 50  $\mu\text{L}$  of the condition. The crystallization robot Mosquito® was used for setting up these smaller drops. A 24 well (4\*6) was used for setting-up the hanging drop of 2  $\mu\text{L}$  (1  $\mu\text{L}$  of protein plus 1  $\mu\text{L}$  of crystallization condition) and the reservoir had 450  $\mu\text{L}$  of a condition. In this case, the drop was manually put on a coverslip. It was inverted on the top of the reservoir and sealed with grease.

### 3. RESULTS

#### 3.1 Cloning

All the domain deletion constructs such as DB-H1-H2, DB-H1-CC, DB-H2-CC, DB-CC and the DNA binding mutant EFCD were cloned under T7 promoter into pHis17 vector with ampicillin resistance. For this purpose, the gene of interest was amplified in the first PCR step (Figure 3.1 A). It was then inserted into the vector by RF PCR method. A double digestion of the plasmid with NdeI and BamHI verified the gene insertion (Figure 3.1 B). The clones were further confirmed by sequencing.

##### A. PCR amplification of gene of interest



##### B. Double digestion check of plasmids with NdeI and BamHI

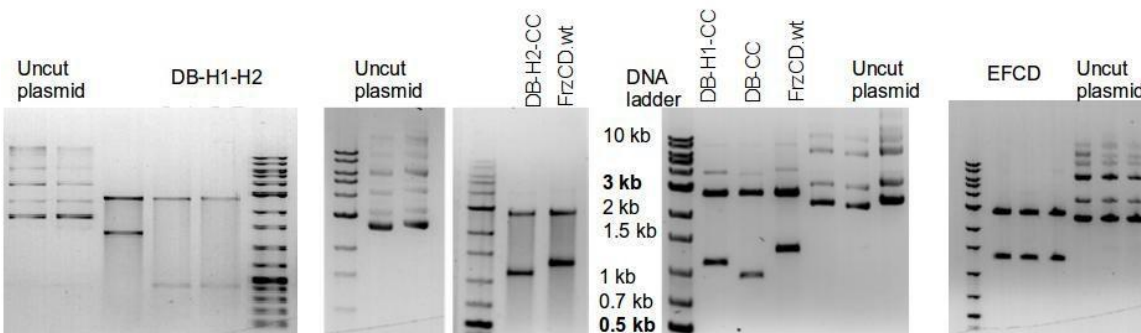
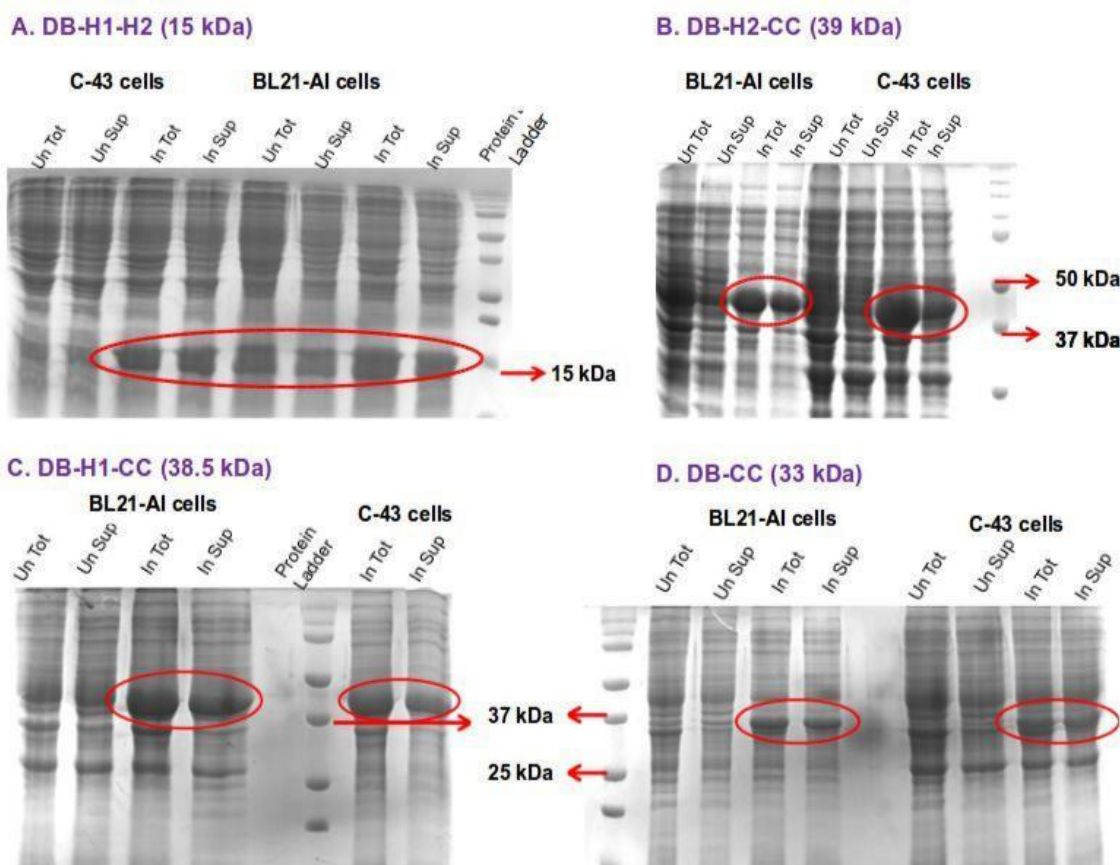


**Figure 3.1: Cloning of all FrzCD constructs.** (A) Initial amplification by PCR-1 at annealing temperature of 56° C and Gradient PCR with varying annealing temperatures (59 - 65° C) for those did not amplify in the first PCR. (B) Double digestion check to verify the insertion of gene of interest to pHis17 vector (2.7 kb). Gene size of FrzCD constructs: FrzCD.wt (1275 bp), DB-H1-H2 (438 bp), DB-H1-CC (1113 bp), DB-H2-CC (1116 bp), DB-CC (964 bp), EFCD (1275 bp).



### 3.2 Overexpression of Proteins

The strains BL21(AI), C43(DE3) and BL21(DE3) of *E. coli* were used to check the protein over-expression. Protein over-expression was checked by comparing the uninduced and induced cells in SDS-PAGE gel. Solubility of the constructs were also seen by comparing if the protein has come to the supernatant fractions by taking gel samples after centrifugation (Figure 3.2 A-F). DB-H1-H2, DB-H1-CC, and DB-CC were well expressed and soluble in both BL21(AI) and C43(DE3) cells. Though DB-H2-CC was also well expressed in both of these strains, the soluble fraction in C43(DE3) was less compared to BL21(AI). EFCD did not show any expression in BL21(AI) cells. Although it showed good expression in C43(DE3), it was in the insoluble fraction. We then tried with BL21(DE3) cells and there was better solubility. We improved on the solubility by growing the culture from a plate incubated for 9 hrs rather than 12 hrs. The culture was induced at  $OD_{600} = 0.6$  with 0.5 mM IPTG and grown for 10 hrs in 18° C post induction.



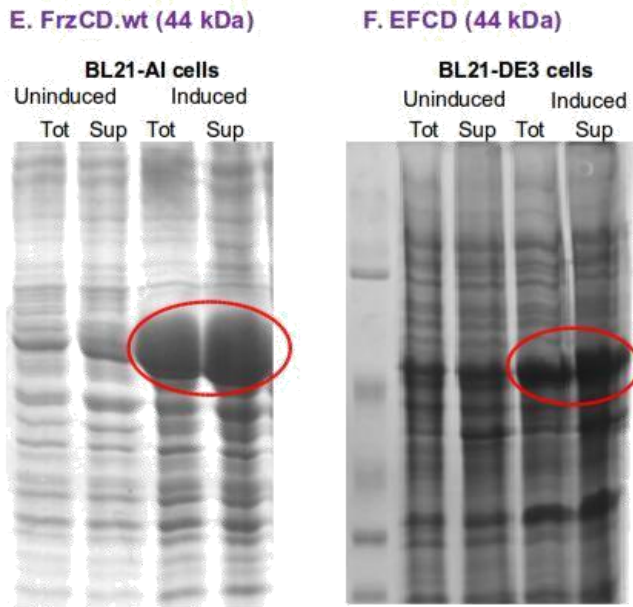


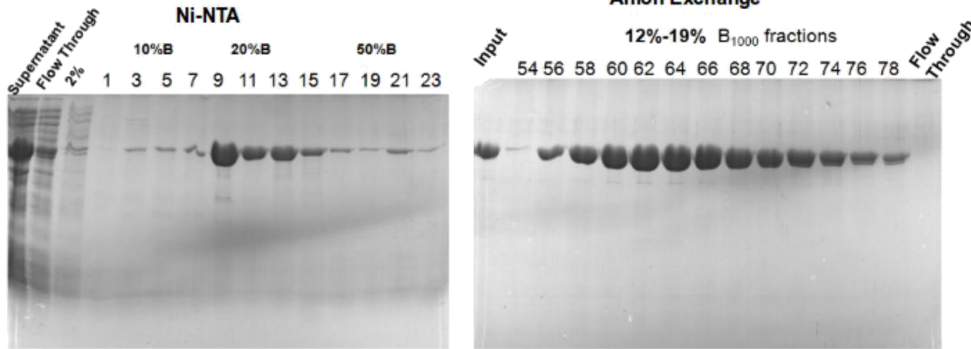
**Figure 3.2 : Protein over-expression of FrzCD constructs (A) DB-H1-H2, (B) DB-H2-CC, (C) DB-H1-CC, (D) DB-CC in BL21-AI cells and C-43(DE3) cells. (E) FrzCD.wt in BL21-AI. (F) EFCD in BL21-DE3 cells. SDS-PAGE gels show the protein bands in Total (Tot) and soluble (Sup) fractions of both uninduced (Un) and induced (In) cells. The over-expression band is marked with red circle.**

### 3.3 Protein Purification

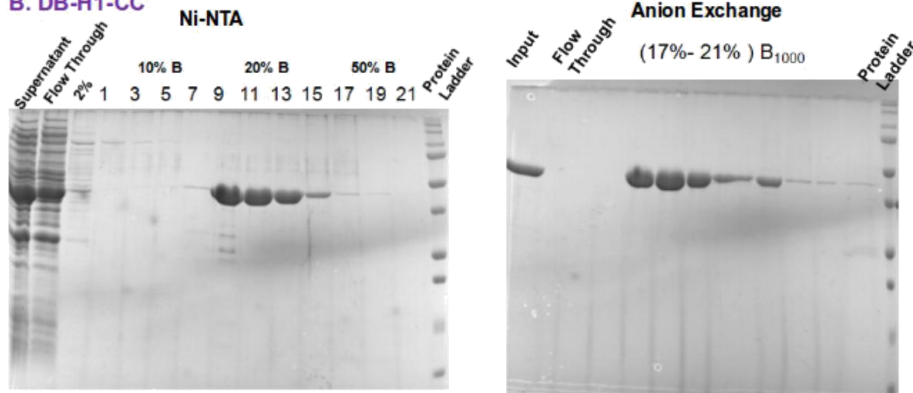
FrzCD.wt, DB-H1-CC, DB-H2-CC, DB-CC, and EFCD were purified by an affinity chromatography step followed by anion exchange column (MonoQ, GE Life Sciences). At each step, the purity was checked by loading onto SDS-PAGE gel (Figure 3.3 A-F). During purification of DB-H1-H2 and EFCD, a lower degradation band was observed after Ni-NTA step itself. For EFCD, we could get rid of that band at least in a few fractions of MonoQ. These fractions were pooled and concentrated, and used for further assays. The lower impurity band of DB-H1-H2 persisted even after the MonoQ step. We did the mass-spectrometry analysis and found out there were two sizes of proteins of 15 kDa and 13 kDa. We suspected the 13 kDa might be degradation from the N-terminal end since it bound to the Ni-NTA, showing the His-tag (at the C-terminal end) is unaffected. The protein was further passed on through a cation exchange column (MonoS, GE Life Sciences). We were able to separate the two bands, presumably because the positively charged N-terminal region bound to the column more strongly. Finally, all the

purified proteins were showing only single band in the SDS-PAGE gel and a single peak in mass-spectrometry corresponding to the expected size.

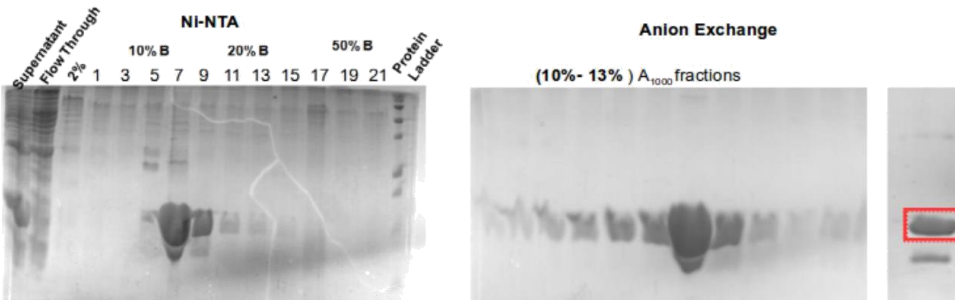
**A. FrzCD wt**



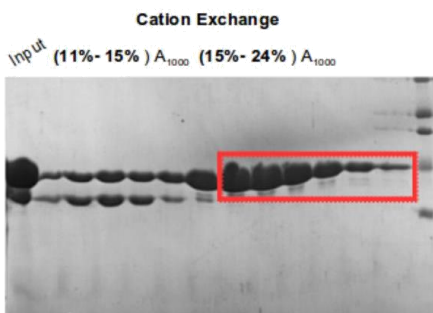
**B. DB-H1-CC**



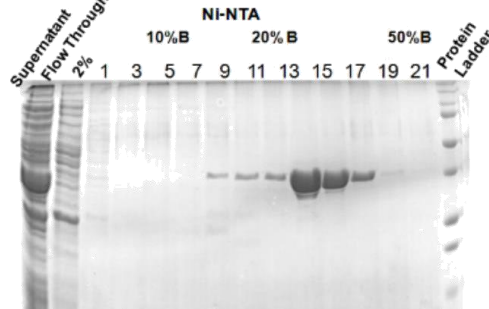
**C. DB-H1-H2**



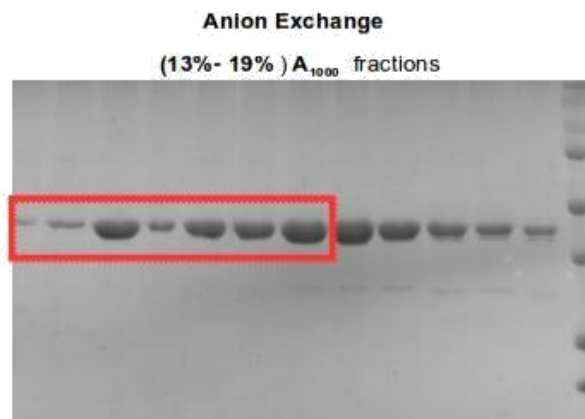
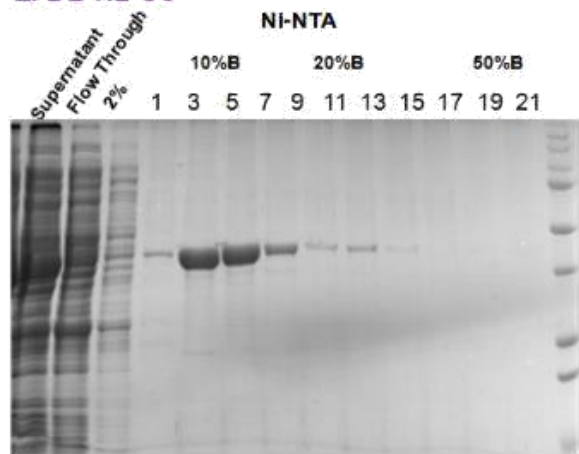
**C. DB-H1-H2**



**D. DB-CC**



### E. DB-H2-CC



### F. EFCD

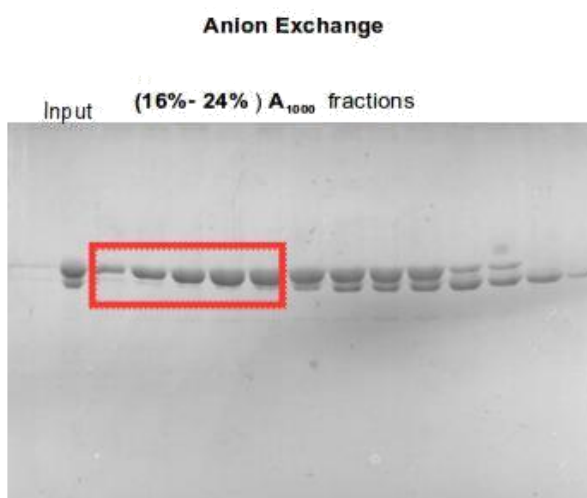
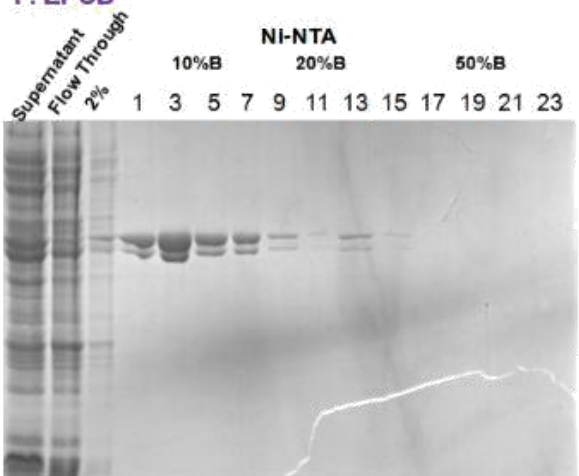


**Figure 3.3 : Protein preparation.** SDS-PAGE gels showing the purity of proteins after Ni-NTA and Mono Q/MonoS columns. Affinity chromatography was done using Ni-NTA column by loading the lysate (supernatant), washing off the impurities (2%B, 5%B) and eluting by step-wise increase in percentage of buffer B (10%, 20%, 50%, 100%). Anion/Cation-Exchange was done by gradient increase in the salt concentration (A1000) by keeping the pH constant at 8.0. The band of interest pooled for concentration of those that had impurities is marked with red box. (A) FrzCD.wt (B) DB-H1-CC (C) DB-H1-H2 (D) DB-CC (E) DB-H2-CC (F) E-FCD.

### 3.4 Protein Oligomerization States

The higher order oligomerization in MCPs might occur due to changes in helix packing and the consequent exposure of domain interfaces. Since HAMP domains are known to be involved in deciding the helix orientation of the coiled-coil domains in MCPs (Airoola, et al., 2007), HAMP domain deleted constructs might form different oligomers compared to wild type. We initiated the characterization of different constructs by checking the oligomeric state under ligand-free conditions.

The oligomerization studies were done using SEC-MALS at 2 mg/ml concentration. FrzCD.wt (44.6 kDa) gave a symmetric peak of 86 kDa corresponding to a dimer (Figure 3.4 A). DB-H1-H2 (15.6 kDa) also had a single asymmetric peak of average molar mass 33 kDa which is also the dimeric size of the protein (Figure 3.4 B). In most cases other than wild-type protein, the elution peaks were asymmetric and constituted of a mixture of oligomeric states (trimer/tetramer). All the other HAMP deletion constructs such as DB-H1-CC, DB-H2-CC, DB-CC eluted in 2 peaks (Figure 3.4 C-G). The prominent peak ~80% mass-fraction consisted of dimers. There was a shorter peak of ~(10-15)% mass-fraction having trimeric/tetrameric size. We checked both DB-H1-CC and DB-CC at 5 mg/ml concentration (Figure 3.4 D,F). For DB-H1-CC, the fraction of protein in the higher molecular weight increased with the increased concentration. A very small fraction of 3% showed a hexameric molecular mass of protein (Figure 3.4 F). A detailed table of protein elution peaks and respective molar mass is given below.

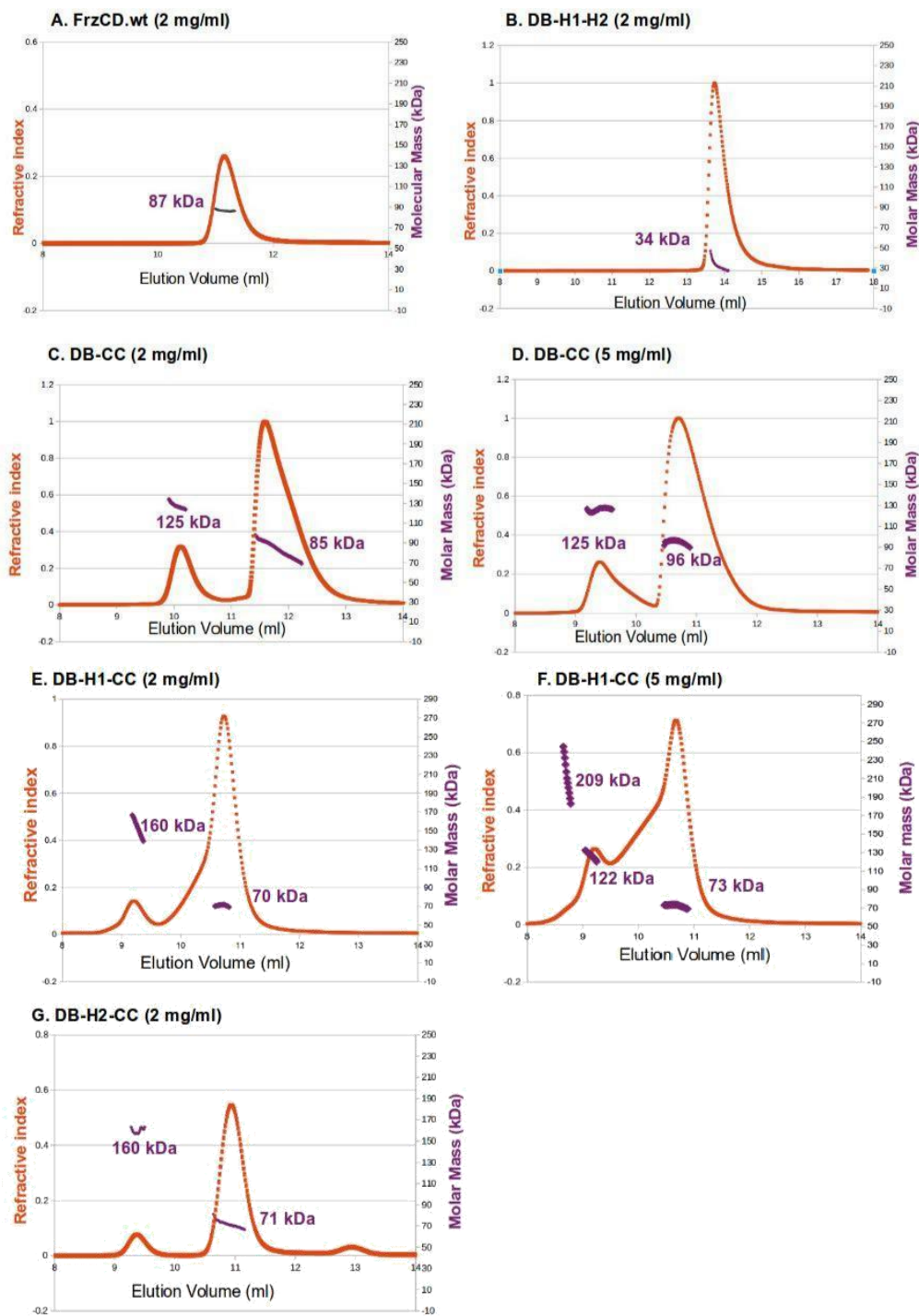


**Figure 3.4: Protein Oligomerization.** SEC-MALS plots showing the Refractive index and Molecular weight of protein corresponding to elution volume from Superdex-200. The average molar mass calculated from Zimm fitting for each peak is written in purple. (A) FrzCD.wt (2 mg/ml), (B) DB-H1-H2 (2 mg/ml), (C) DB-CC (2 mg/ml), (D) DB-CC (5 mg/ml), (E) DB-H1-CC (2 mg/ml) (F) DB-H1-CC (5 mg/ml), (G) DB-H2-CC (2 mg/ml)

**Table 3.1:** Molar mass estimation from SEC-MALS

Name of Construct	Concentration (mg/ml)	Molar mass of monomer (kDa)	Oligomeric state of construct	Peak (mass-fraction under the peak)	Average molar mass $M_{avg}$ (kDa)	$M_n$ (kDa)	$M_p$ (kDa)	$M_w$ (kDa)	$M_z$ (kDa)	$M_{(z+1)}$ (kDa)
FrzCD.wt	2	44.6	Dimer	1 (100%)	86.5	86.3	86.4	86.3	86.3	86.3
DB-H1-H2	2	15.6	Dimer	1 (100%)	33.9	34.6	34.6	39.2	–	–
DB-CC	2	33	Trimer/ Tetramer	1 (83%)	84.7	87	91.5	87.7	88.4	89.2
				2 (17%)	125.2	125.7	125.2	125.3	125.3	125.2
DB-CC	5	33	Trimer/ Tetramer	1 (81%)	95.5	94.6	96	94.6	94.7	94.7
				2 (19%)	125.3	125.9	127.2	125.9	125.3	125.3
DB-H2-CC	2	39	Dimer/ Tetramer	1 (91 %)	70.7	69.9	70.8	70.7	72.6	77.3
				2 (9%)	159.8	166.9	157.6	169.1	172.4	177.4
DB-H1-CC	2	38.5	Dimer/ Tetramer	1 (86%)	74.4	73.2	74.7	73.3	73.4	73.5
				2 (14%)	148.1	145.1	147.5	146.8	147.6	148.1
DB-H1-CC	5	38.5	Dimer/ Trimer/ Hexamer	1 (76%)	72	73.5	72	72.1	72.1	72.6
				2 (21%)	121.2	123.5	121.6	122.1	122.6	121.9
				3 (3%)	208.7	226.1	182.7	232.7	240	248

### 3.5 DNA Binding Assays

FrzCD was shown to co-localize with the nucleoid *in vivo* (Moine, et al., 2017). Transmembrane MCPs generally form a 'trimer of dimers' assembly on the membrane (Briegel, et al., 2011). FrzCD being a cytoplasmic MCP does not interact with the membrane to form such an assembly. We propose that it might be forming a hexameric array by using DNA as a scaffold. After making all the domain deletion constructs, we wanted to check whether the protein is functional. The DNA-binding activity of the constructs was checked by a 429 bp DNA. Following this, DNA of shorter lengths were used to compare between the various constructs, and also to design an appropriate DNA substrate for crystallization. Smaller lengths of DNA is preferred for crystallization purposes. We thought of checking the binding of all the constructs with smaller DNA sizes. Oligonucleotides for forming dsDNA of sizes of 69 bp, and 35 bp were available in the lab, and used for the studies. These sizes were also compatible with carrying out the EMSA studies on agarose gel.

DNA binding assays were done for all the constructs mainly with 429 bp, 69 bp, and 35 bp DNA. The coiled-coil deletion construct DB-H1-H2 showed a decreased shift of DNA in the gel (Figure 3.5 – 3.7). For the DNA binding mutant EFCD, the mobility of DNA with protein and naked DNA was same indicating no binding. FrzCD.wt, DB-H1-CC, DB-H2-CC and DB-CC exhibited a complete shift for the DNA for 10  $\mu$ M of protein. Although DB-H1-H2 was not able to show much retardation for smaller DNAs of 429 bp, 69 bp, and 35 bp length, it was able to show a significant shift for a plasmid DNA of ~3.2 kb in agarose gel (Figure 3.8).



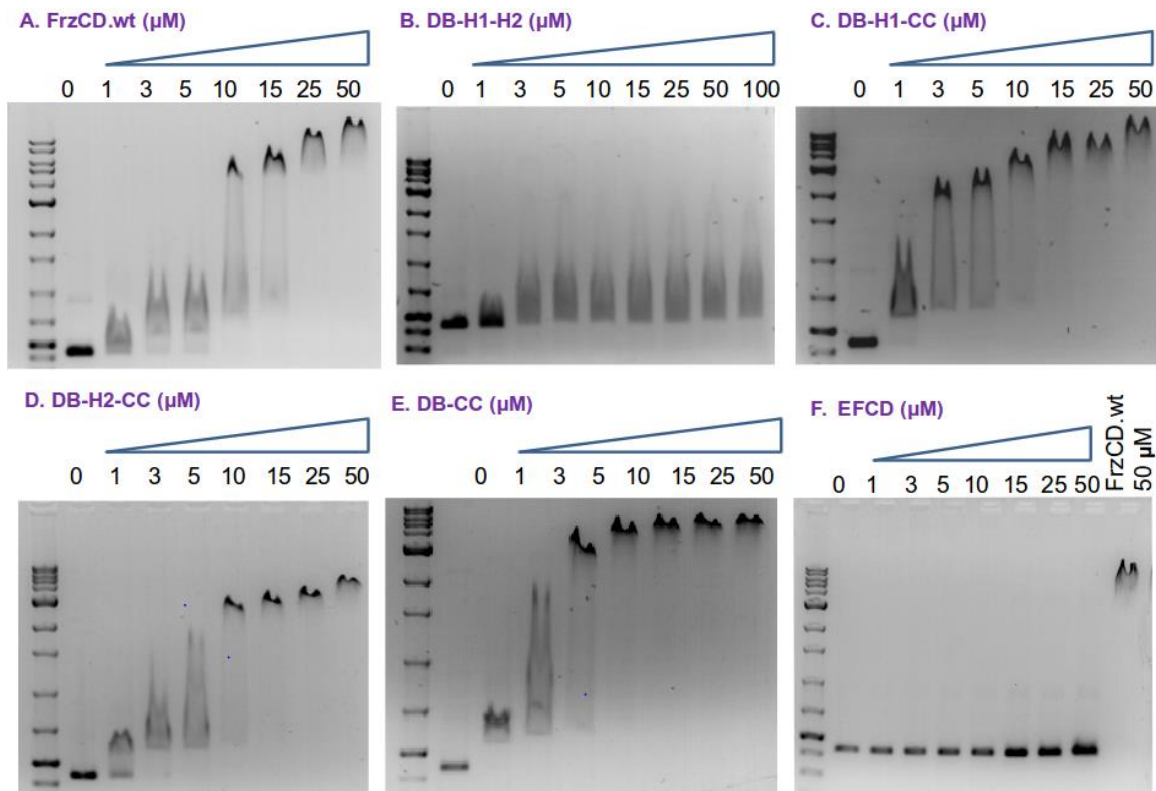


**Figure 3.5: DNA- binding assays with 429 bp DNA.** EMSA performed in 1.5% Agarose gel showing the shift of DNA with increasing protein concentration. 40 nM of DNA was incubated in different protein concentrations (0-50  $\mu\text{M}$ ) for 30 min before loading on the gel. (A) FrzCD.wt, (B) DB-H1-H2, (C) DB-H1-CC (D) DB-H2-CC (E) DB-CC (F) EFCD.

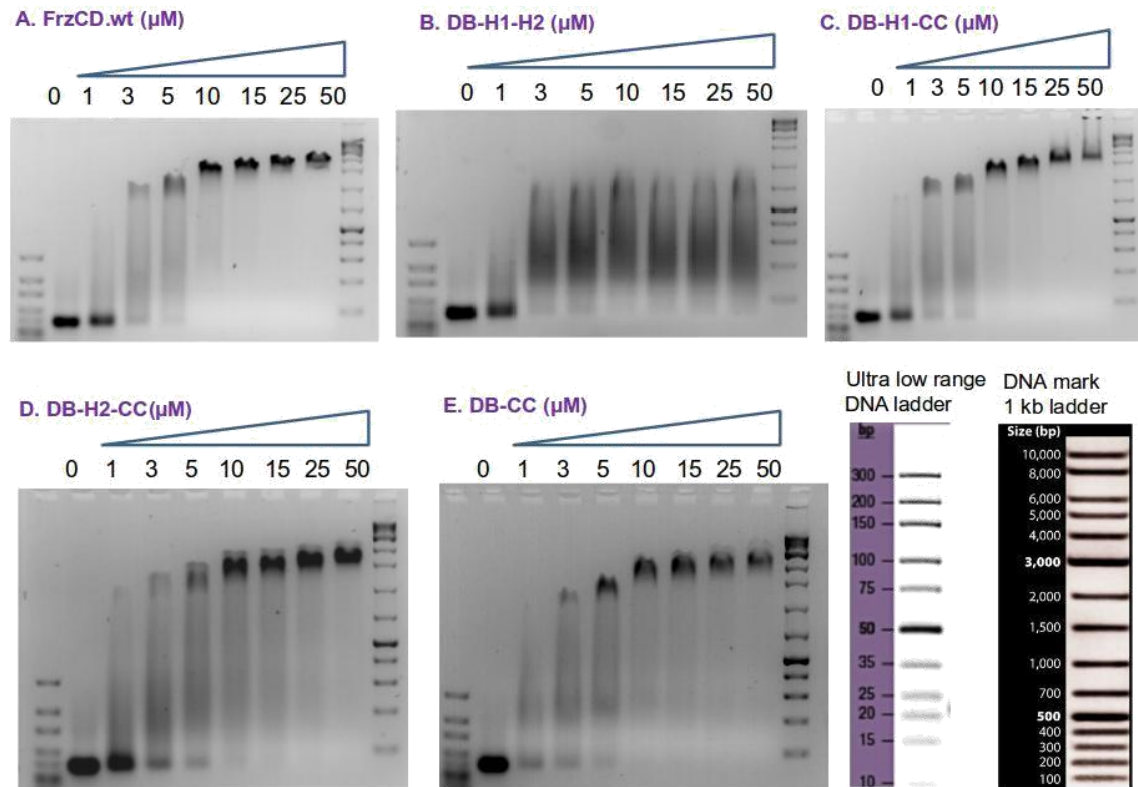


**Figure 3.6: DNA- binding assays with 69 bp DNA.** A 2.5% agarose gel shows the retardation in mobility of protein bound DNA compared to free DNA. 500 nM of DNA incubated with 0-50 nM protein concentrations. (A) FrzCD.wt, (B) DB-H1-H2, (C) DB-H1-CC (D) DB-H2-CC (E) DB-CC. Ultra low range DNA ladder and DNA mark 1 kb ladder are loaded on either sides to show the shift. (F) Band sizes for the DNA ladders (Adapted from the manufacturer's website).

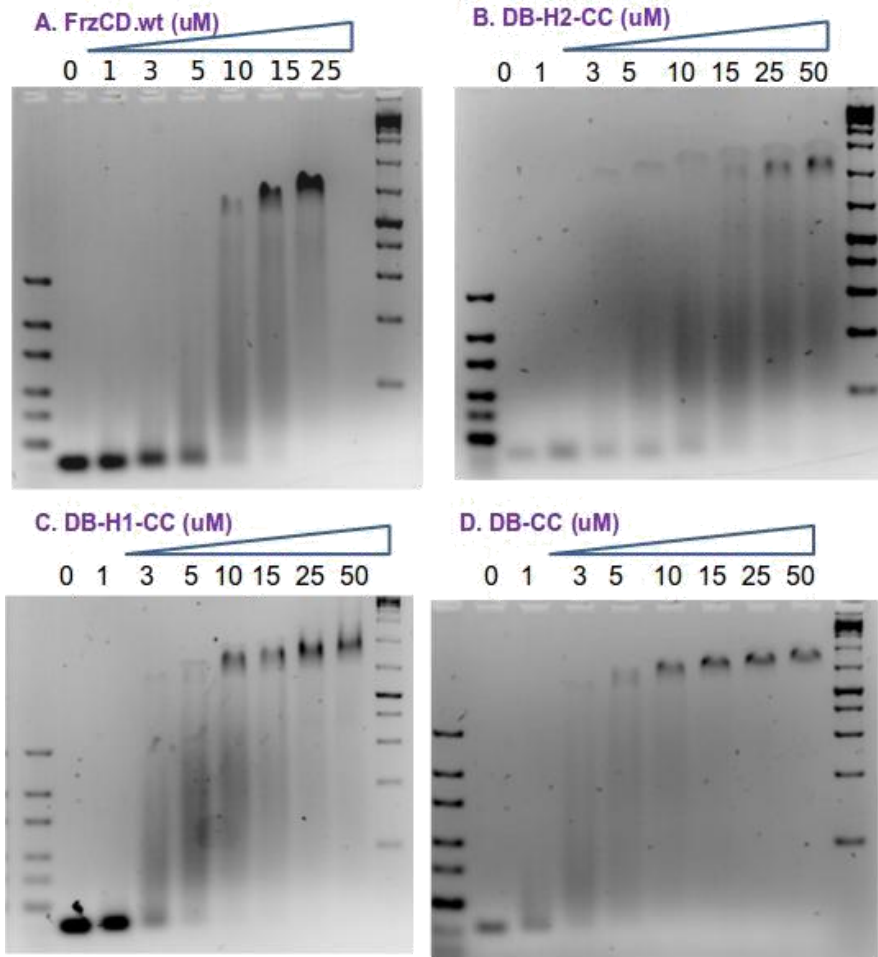


**Figure 3.7: DNA- binding assays with 35 bp DNA.** EMSA gel showing the retardation in mobility of 1000 mM of 35 bp DNA in 3.5 % agarose gel. A maximum shift of upto 1 kb is observed for all the constructs (A) FrzCD.wt, (B) DB-H2-CC, (C) DB-H1-CC, (D) DB-CC.

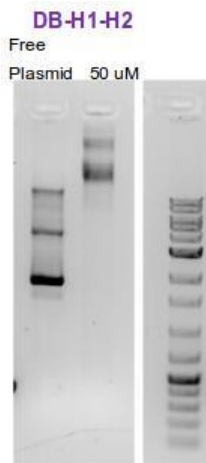


**Figure 3.8: DNA- binding assay of DB-H1-H2 with plasmid DNA.** 1% agarose gel showing the binding of DB-H1-H2 with a plasmid DNA of 3.2 kb

### 3.5 Crystallization trials of FrzCD.wt :

The wild-type protein was giving needle-like clusters in the initial screens. We started with optimizing those hits by varying the concentration of the precipitant, pH of buffer and trying different additive screen conditions. The various conditions used for optimizing the crystal quality are listed in a table (Table 3.2). After many optimization screens, we got a condition having Li<sub>2</sub>SO<sub>4</sub>-0.3 M, Heparin 3%, PEG 4K 7% and we managed to get hexagonal shaped crystals (Figure 3.9). But it did not give any diffraction data. We are still optimizing on more conditions and cryo-protectant to improve the quality of crystals.

**Table 3.2:** Crystallization conditions

Screen Name	Precipitant Mix	Additional Variants	Buffer (0.1M Tris) pH	Protein Concentration (mg/ml) Ratio of Protein:condition
OS-4A	Li <sub>2</sub> SO <sub>4</sub> , (0.05-0.3) M PEG 4K, (5-20)%		8 8.5	6 (1:1) 8 (1:1)
OS-4B	Li <sub>2</sub> SO <sub>4</sub> , (0.05-0.3) M Jeffamine,(10-30)%		8 8.5	6 (1:1) 8 (1:1)
OS-5	Li <sub>2</sub> SO <sub>4</sub> , 0.3 M PEG 4K, 10%	Additive screen - HT HR2-138	8.5	6 (1:1)
OS-6	Li <sub>2</sub> SO <sub>4</sub> , 0.2 M Jeffamine, 20%	Additive screen – HT HR2-138	8.5	6 (1:1)
OS-7	Li <sub>2</sub> SO <sub>4</sub> , 0.3 M PEG 4K, 10%	1.Spermine-tetrachloride 2.Heparin 3.1-Butanol 4.1-Propanol 5.Isopropanol 6.Isoamyl Alcohol	8.5	6 (1:1)

Screen Name	Precipitant Mix	Additional Variants	Buffer (0.1M Tris) pH	Protein Concentration (mg/ml) Ratio of Protein:condition
OS-8	Li <sub>2</sub> SO <sub>4</sub> , 0.2 M Jeffamine, 20%	1.Spermine-tetrachloride 2.Heparin 3.1-Butanol 4.1-Propanol 5.Isopropanol 6.Isoamyl Alcohol	8.5	6 (1:1)
OS-9	Li <sub>2</sub> SO <sub>4</sub> , 0.3 M PEG 4K, 10%	Heparin (2.5%, 4%,7%)	8.5	6 (1:1, 1:2, 2:1) 8 (1:1,1:2,) 10 (1:1,1:2,)
OS-10	Li <sub>2</sub> SO <sub>4</sub> , 0.2 M Jeffamine, 20%	Isoamyl Alcohol (11%, 13%, 15%)	8.5	6 (1:1, 1:2, 2:1) 8 (1:1,1:2,) 10 (1:1,1:2, )
OS-11	Li <sub>2</sub> SO <sub>4</sub> , 0.3 M 10% PEG 4K	1- Propanol (13%, 15%, 17%)	8.5	6(1:1, 1:2, 2:1) 8 (1:1,1:2,) 10 (1:1,1:2, )
OS-12 A	Li <sub>2</sub> SO <sub>4</sub> , 0.3 M PEG 4K, 10%	1. Heparin, (4-9)% 2. Spermine tetrachloride, (2.5- 20) mM		6 (1:1)
OS-13 Hanging drop	Li <sub>2</sub> SO <sub>4</sub> , 0.3 M PEG 4K, 10%	Heparin, (3, ,5, 6, 7)%	8.5	6 (1:1, 1:2)
OS- 14	Li <sub>2</sub> SO <sub>4</sub> , (0.15-0.25) M Jeffamine, (15-25)%	Spermine tetrachloride, (2.5-30) mM	8.5	6(1:1)
OS-15	Li <sub>2</sub> SO <sub>4</sub> , (0.2-0.4) M PEG 4K, (7-15)%	Spermine tetrachloride, (2.5-30) mM	8.5	6 (1:1)
OS-16 Hanging drop	Li <sub>2</sub> SO <sub>4</sub> , (0.2, 0.25) M Jeffamine, (20, 25)%	Spermine tetrachloride, (15- 20) mM	8.5	6 (1:1, 1:2)
OS-17 Hanging drop	Li <sub>2</sub> SO <sub>4</sub> , (0.3, 0.4) M PEG 4K, (7, 10)%	Spermine (17-22) mM	8.5	6 (1:1, 1:2)

Screen Name	Precipitant Mix	Additional Variants	Buffer (0.1M Tris) pH	Protein Concentration (mg/ml) Ratio of Protein:condition
	(0.2, 0.25) M Jeffamine (20, 25)%	(3, ,5, 8)%		
OS-18 B	Li <sub>2</sub> SO <sub>4</sub> , (0.3, 0.4) M PEG 4K, (7, 10)%	Heparin, (3, ,5, 8)%	8.5	6 (1:1, 1:2)
OS-19 A	Li <sub>2</sub> SO <sub>4</sub> , (0.3, 0.4) M PEG 4K, (10)%	1,3- propanediol, (3-18)%	8.5	6 (1:1, 1:2)
OS-19 B	Li <sub>2</sub> SO <sub>4</sub> , (0.2, 0.3) M Jeffamine, (20, 25)%	1,3- Propanediol, (3-18)%	8.5	6 (1:1, 1:2)
OS-20 A	Li <sub>2</sub> SO <sub>4</sub> , (0.3, 0.4) M PEG 4K, (10)%	1,2- Butanediol, (3-18)%	8.5	6 (1:1, 1:2)
OS-20 B	Li <sub>2</sub> SO <sub>4</sub> , (0.2, 0.3) M Jeffamine, (20, 25)%	1,2- Butanediol, (3-18)%	8.5	6 (1:1, 1:2)
OS-21 A	Li <sub>2</sub> SO <sub>4</sub> , (0.3, 0.4) M PEG 4K, (10)%	1,2- propanediol, (3-18)%	8.5	6 (1:1, 1:2)
OS-21 B	Li <sub>2</sub> SO <sub>4</sub> , (0.2, 0.3) M Jeffamine, (20, 25)%	1,2-propanediol, (3-18)%	8.5	6 (1:1, 1:2)
OS-22	Li <sub>2</sub> SO <sub>4</sub> , (0.3, 0.35) M PEG 4K, (7, 10)%	Heparin, (3, 4)%	8.5	6 (1:1, 1:2)
OS-26	Li <sub>2</sub> SO <sub>4</sub> , 0.3 M PEG 4K, 6%	Heparin, 3 %	8 8.5 9	6 (1:1, 1:2)
OS-27	Li <sub>2</sub> SO <sub>4</sub> , 0.3 M Heparin, 3 %	PEG 3.5K, (7-20) %	9	6 (1:1, 1:2)

Screen Name	Precipitant Mix	Additional Variants	Buffer (0.1M Tris) pH	Protein Concentration (mg/ml) Ratio of Protein:condition
OS-28	Li <sub>2</sub> SO <sub>4</sub> , 0.3 M Heparin, 3 % PEG 4K, 7%	Additive screen - HT HR2-138	9	6 (1:1, 1:2)
OS-29	Li <sub>2</sub> SO <sub>4</sub> , 0.3 M Heparin, 3 % PEG 4K, 7%	Silver Bullets (Hampton)	9	6 (1:1, 1:2)
OS-30	Li <sub>2</sub> SO <sub>4</sub> , 0.3 M Heparin, 3 % PEG 4K, 7%	Spermine tetrachloride, (0.5 – 12) mM Jeffamine (1-10)%	9	6 (1:1)
OS-31	Li <sub>2</sub> SO <sub>4</sub> , 0.3 M Heparin, 3 % PEG 4K, 7%	Spermine tetrachloride, (10 - 18) mM Jeffamine , (10-15)%	9	6 (1:1)
OS-32	Li <sub>2</sub> SO <sub>4</sub> , 0.3 M Heparin, 3 % PEG 4K, 7%		8 8.5 9	6 (1:1)

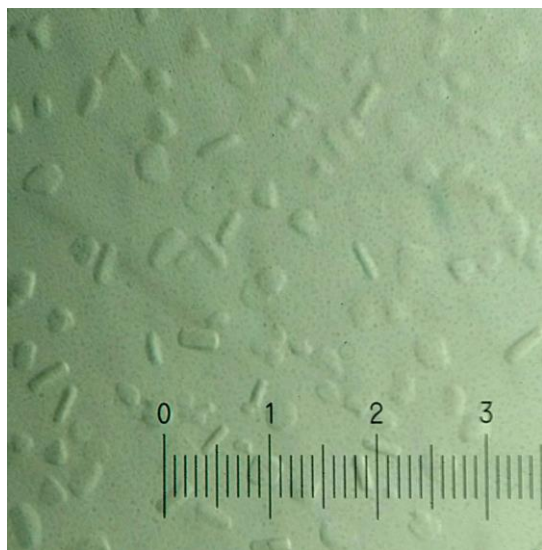


**Figure 3.9: Crystals of FrzCD.**

Hexagonal shaped crystals of FrzCD.wt  
(1 unit in the scale corresponds to 8 μm)

## 4. DISCUSSION

Two halves of the linker region between DNA-binding and coiled coil domains of FrzCD aligned well with HAMP domain sequences. We could find the presence of two HAMPs continuous to each other from secondary structure prediction analysis also. We made the domain deletion constructs to get insights into the structural and functional role of each domain. MCPs are long coiled-coil homodimeric proteins which generally form functional units consisting of trimer of dimers in the presence of membrane. We propose that FrzCD might be forming a hexameric array by using DNA as a scaffold, instead of membrane. Hence, oligomerisation studies and DNA binding assays were carried out with the various domain deletion constructs of FrzCD.

### Oligomerization studies of FrzCD constructs:

All the protein constructs were subjected to SEC-MALS to get a reliable molar mass of the protein in solution which indicates the oligomeric state of the protein. FrzCD.wt gave a symmetric peak corresponding to a dimer (Table 3.1). The coiled-coil deletion construct, DB-H1-H2 also eluted in a single peak as a dimer (Table 3.1). This suggests that HAMP domains are sufficient for dimerization of the protein and coiled-coil domain is not a necessary condition for dimerization.

For the other constructs where HAMP domains were deleted, 10-20 % mass-fraction of a higher oligomeric state was also observed along with the major dimeric peak (80-90% mass-fraction). In the absence of both of the HAMP domains (DB-CC), the protein showed an additional trimeric state. In the absence of any one of the HAMPs (DB-H1-CC and DB-H2-CC), it was found to be a mixture of dimeric and tetrameric states. All these reveal that the presence of both the HAMP domains holds the protein in a dimeric form or restricts it from forming higher order oligomers under ligand-free conditions. This suggests that the orientation of coiled-coil domain might be a determinant of the oligomeric state of protein because these domains may be in different conformations when a linker domain is removed. In a ligand-free state, the HAMP domains may be



required for constraining the coiled coil helices in a particular orientation that is compatible with only a dimeric species.

All the initial SEC-MALS runs were done at 2 mg/ml concentration of the protein. Since DB-CC, DB-H1-CC and DB-H2-CC showed a higher oligomeric peak, we suspected that the proteins might form higher oligomers at higher concentration. Coiled coil proteins are reported to show a concentration dependent dynamic oligomeric behaviour (Dewangan, et al., 2017). In order to verify this, we repeated the same experiment with DB-CC and DB-H1-CC at 5 mg/ml concentration. DB-CC did not show any difference and resulted in two peaks of dimer and trimer similar to the previous results. The profile of DB-H1-CC was markedly different. It showed a 10 % decrease in the proportion of dimeric state. The 86 % of mass-fraction was previously dimers at 2 mg/ml, and when the concentration was increased to 5 mg/ml it changed to 76% of dimers, 21% of trimers and 3% of hexamers. For concluding if there is a real hexamer formation, we are planning to perform the same at even higher concentrations.

### DNA binding properties:

Among all the FrzCD constructs, DB-H1-H2, the coiled-coil deletion construct, showed the least affinity in DNA binding experiments. DB-H1-H2 was showing a smeary shift rather than a complete shift of the DNA indicating the protein-DNA complex is less stable. This observation was consistent with the study where they made FrzCD $\Delta$ 131-147 construct which showed lower efficiency for DNA binding (Moine et al., 2017). The fact that DB-H1-H2 is not able to form a stable complex, though the DNA-binding region is intact, highlights the significance of coiled-coil in the formation of a stable protein-DNA complex. For EFCD, where the N-terminal positively charged residues (arginines and lysines) are mutated to glutamates, the EMSA gel did not show any shift or a smearing. This implies the complete loss of DNA-binding activity of the protein and reveals that these residues are determinants of the DNA-binding activity. The comparison of the EFCD and DB-H1-H2 DNA binding assays suggests that the stability

of the dimeric complex or higher order oligomers is affected in DB-H1-H2, and, and this may be essential for forming a stable complex with DNA.

Binding assays for all the constructs were done with 429 bp, 69 bp, and 35 bp double-stranded DNA. For the 429 bp, DNA shift in the gel begins at 1  $\mu$ M of the protein itself (Figure.3.5). In the case of 69 bp DNA, the shift is seen between 3  $\mu$ M - 5  $\mu$ M of protein concentration (Figure.3.6). As we went to a lower DNA length of 35 bp, the DNA shift was seen only from 5  $\mu$ M - 10  $\mu$ M of protein (Figure.3.7). This clearly suggests that the protein has more affinity towards longer DNA. Interestingly, DB-H1-H2, which could not make a complete shift for any of these three sizes of DNA, was able to bind reasonably with a plasmid DNA of  $\sim$  3.2 kb in the gel (Figure 3.8). However, a comparison between circular and linear DNA of the same size has not been carried out yet.

If we compare the binding pattern for 429 bp DNA across different constructs, all of them except DB-H1-H2 were able to shift the DNA in the gel. Though this experiment has been performed only once for the DB-H1-H2 and 429 bp DNA, similar results have been obtained for other DNA lengths also with the DB-H1-H2 construct. Binding assays with 69 bp DNA were done in triplicates and the results observed were very consistent. In the 2.5% agarose gel, FrzCD.wt, DB-H1-CC, DB-CC, and DB-H2-CC shifted the DNA similarly to a maximum of around 2.5 kb (Figure .3.6). Since the migration of DNA in the same gel can be affected by the size and shape factors, we suspect that upon binding to DNA, the proteins may be forming the same higher order oligomer. These interactions for higher order oligomerization might be mediated by the coiled-coil region. All the proteins could shift the 35 bp DNA to a maximum of 1 kb at 50  $\mu$ M of protein (Figure 3.7). These assays were done only once and has to be repeated for further analysis, and quantification.

The presence of two HAMP domains with two flexible linkers between the amphipathic helices might be blocking the oligomerization interface under DNA-free conditions. The binding to DNA might lead to a different orientation of HAMPs leading to the exposure of oligomerization interfaces of the constructs (FrzCD.wt, DB-H1-CC, DB-H2-CC, DB-CC). Hence, these may form similar higher order assemblies despite the presence or absence of HAMP domain. This can be a possible explanation for the formation of similar shifts in the DNA-binding assay of FrzCD.wt, DB-H1-CC, DB-H2-CC, DB-CC constructs.

For obtaining better diffracting crystals, we have to do more screens and work on cryo-protectant optimization. In general, it is difficult to get well-diffracting crystals for coiled-coil proteins, which can be observed from the low number of crystal structures of coiled-coil domains of MCPs. The progress from needle-shaped crystals to hexagonal crystals is promising in this direction, and further trials are being carried out in the lab currently.

In summary, the oligomerisation and DNA binding studies for the different domain combinations of FrzCD appear to suggest that the HAMPs and the coiled coil domains contribute to specific oligomerisation features, which in turn is required for stability of the FrzCD-DNA complex. There is a length-dependence for binding affinities of all the constructs. Binding to the DNA may result in the formation of higher order assemblies, which has to be confirmed by further experiments.

## 5. CONCLUSION AND FUTURE PROSPECTS

The domain architecture of the protein was proposed as a N-terminal DNA binding region, two continuous HAMP domains and the C-terminal coiled-coil domain. In order to understand the role of HAMP domain in FrzCD, different constructs for the protein was designed by systematically deleting each domain. The domain deletion constructs DB-H1-H2, DB-CC, DB-H1-CC, DB-CC and the DNA binding mutant EFCD were cloned into the pHis17 vector. When over-expressed, all of these came into the soluble fraction. These were purified using affinity chromatography followed by an ion exchange column and mass-spectrometry was done to confirm the molecular mass of the constructs. Protein oligomeric studies were carried out for the all domain deletion constructs. None of the constructs were found to form aggregates. The coiled-coil domain was found to be involved in the formation of a higher oligomeric state. The presence of two HAMP domain was found to restrict the protein in the dimeric form. DNA binding assays have shown that all the constructs show more affinity towards longer DNA. Coiled-coil domain is necessary for the formation of a stable complex of protein and DNA. Binding assay with EFCD has shown the five positively charged residues are responsible for DNA binding. Crystallization trials have progressed from needles to hexagonal shaped small crystals.

To confirm the dynamic behavior of HAMP deletion constructs, we are planning to perform SEC-MALS with a higher concentration of protein. We are also planning to analyze the protein-DNA complex by SEC-MALS to verify if the protein is forming more stable higher order oligomers upon DNA binding. The preliminary standardizations of the buffer where the complex can be stable for this are in progress by using SEC column. So far, we have done only the qualitative analysis of DNA binding. For the quantitative analysis and calculating the  $K_d$  of binding, we are planning to perform fluorescence anisotropy experiments for DNA-protein interaction by labeling the DNA. FrzCD is a system with only single tryptophan in the HAMP2 of the protein. Intrinsic Tryptophan Fluorescence assays can also tell if there is a change in oligomerization of the protein when bound to DNA.

## 6. REFERENCES

- Airola, M. V, Watts, K.J., Bilwes, A.M., and Crane, B.R. (2010). Article Structure of Concatenated HAMP Domains Provides a Mechanism for Signal Transduction. *Struct. Des.* 18, 436–448.
- Alexander, R. (2007). Evolutionary genomics of methyl-accepting chemotaxis proteins. (PhD Thesis)
- Briegel, A., Li, X., Bilwes, A.M., Hughes, K. T., Jensen, G.J., and Crane, B.R. (2011). Bacterial chemoreceptor arrays are hexagonally packed trimers of receptor dimers networked by rings of kinase and coupling proteins. *PNAS* 109, 3766–3771.
- Bustamante, V.H., Martínez-Flores, I., Vlamakis, H.C., and Zusman, D.R. (2004). Analysis of the Frz signal transduction system of *Myxococcus xanthus* shows the importance of the conserved C-terminal region of the cytoplasmic chemoreceptor FrzCD in sensing signals. *Mol. Microbiol.* 53, 1501–1513.
- Dewangan, P.S., Sonawane, P.J., Chouksey, A.R., and Chauhan, R. (2017). The Nup62 Coiled-Coil Motif Provides Plasticity for Triple-Helix Bundle Formation. *Biochemistry* 56, 2803–2811.
- van den Ent, F., and Löwe, J. (2006). RF cloning: A restriction-free method for inserting target genes into plasmids. *J. Biochem. Biophys. Methods* 67, 67–74.
- Gushchin, I., Melnikov, I., Polovinkin, V., Ishchenko, A., Yuzhakova, A., Buslaev, P., Bourenkov, G., Grudin, S., Round, E., Balandin, T., et al. (2017). Mechanism of transmembrane signaling by sensor histidine kinases. *Science* 356, 1–12.
- Guzzo, M., Agrebi, R., Espinosa, L., Baronian, G., and Molle, V. (2015). Evolution and Design Governing Signal Precision and Amplification in a Bacterial Chemosensory Pathway. *PLoS Genet* 11.

Hall, B.A., Armitage, J.P., and Sansom, M.S.P. (2012). Mechanism of Bacterial Signal Transduction Revealed by Molecular Dynamics of Tsr Dimers and Trimers of Dimers in Lipid Vesicles. *PLoS Comput Biol* 8.

Moine, A., Espinosa, L., Martineau, E., Yaikhomba, M., Jazleena, P.J., Byrne, D., Biondi, E.G., Notomista, E., Brilli, M., Molle, V., et al. (2017). The nucleoid as a scaffold for the assembly of bacterial signaling complexes. *PLoS Genet* 13.

Shi, W., Kohler, T., and Zusman, D.R. (1993). Chemotaxis plays a role in the social behaviour of *Myxococcus xanthus*. *Mol Microbiol* 9, 601–611.

Wadhams, G.H., and Armitage, J.P. (2004). Making sense of it all: bacterial chemotaxis. *Nat. Rev. Mol. Cell Biol.* 5, 1024–1037.

